JTTEE5 14:91-99
DOI: 10.1361/10599630522774
1059-9630/$19.00 © ASM International

New Attachment for Controlling Gas Flow in the HVOF Process

A. Dolatabadi, V. Pershin, and J. Mostaghimi

(Submitted September 15, 2003; in revised form November 1, 2004)

During the decade, the high-velocity oxyfuel (HVOF) process proved to be a technological alternative to the many conventional thermal spray processes. It would be very advantageous to design a nozzle that provides improved performance in the areas of deposition efficiency, particle in-flight oxidation, and flexibility to allow deposition of ceramic coatings. Based on a numerical analysis, a new attachment to a standard HVOF torch was modeled, designed, tested, and used to produce thermal spray coatings according to the industrial needs mentioned above. Performance of the attachment was investigated by spraying several coating materials including metal and ceramic powders. Particle conditions and spatial distribution, as well as gas phase composition, corresponding to the new attachment and the standard HVOF gun, were compared. The attachment provides better particle spatial distribution, combined with higher particle velocity and temperature.

Keywords air entrainment, HVOF, particle conditions, shroud attachment, spatial distribution

1. Introduction

The high-velocity oxyfuel process (HVOF) has been demonstrated to be one of the most efficient techniques for depositing high-performance coatings at moderate cost. In this process, a mixture of fuel and oxygen ignites in a high-pressure combustion chamber, and the combustion products are accelerated through a converging-diverging nozzle (Fig. 1). As a result, injected particles attain high velocity at a relatively low temperature. High particle kinetic energy upon impact leads to formation of dense, well-adhered coating, whereas reduced temperature prevents extensive oxidation of particles.

Although the HVOF process was shown to be technologically advanced in comparison to other thermal spray processes, there are some areas that can be improved to achieve optimum performance. These can be categorized into the following three issues.

Any thermal spray process in the ambient atmosphere is accompanied by air entrainment into a jet, which usually results in in-flight metal particle oxidation. It is important to minimize oxidation during coating deposition, which improves overall coating performance (Ref 1, 2). Vacuum plasma spraying (VPS) allows elimination of oxygen in the spraying region and provides low oxide coatings, but this process is expensive and time consuming and has restrictions on the size of coated parts by the size of the vacuum chamber (Ref 3). Compared with other spraying processes, oxidation rate during the HVOF spraying is one of the lowest, and in some cases, it is comparable with that of VPS coatings (Ref 4, 5). To use the HVOF process as an alternative to the VPS, air entrainment should be minimized.

Oblique shocks are present; Fig. 2 illustrates velocity fluctuation of a single particle leaving an HVOF gun and passing through the first shock wave outside of the nozzle. Additionally, particle trajectory deviation due to interaction with these oblique shocks also has been observed. Provided that a particle passes a number of shocks until it reaches a substrate located up to 30 cm far from the nozzle, deposition of such a deviated particle with low kinetic and thermal energy will negatively affect coating quality (Ref 11). Another disadvantage of the HVOF technique relates to the types of materials that can be deposited. Due to the limited flame temperatures, short particle in-flight times HVOF is inefficient for deposition of a majority of ceramic coatings.

Attaching a protective shroud to the end of the HVOF nozzle to delay the jet mixing with air may be a feasible solution to address the aforementioned disadvantages (Ref 6, 7). In an attempt to reduce the oxygen content in the HVOF coatings, Moskowitz et al. (Ref 8) tested a cylindrical shroud with additional inert gas injection. They claimed that the shrouded nozzle produces low-oxide coatings. The present authors analyzed the effect of this type of the shroud on in-flight particle conditions and coatings formation (Ref 9, 10). The authors' experiments and numerical simulations of the design, similar to those presented in Ref 8, showed that attaching a cylindrical shroud produces coatings with lower oxygen contents compared with that of the unconfined jet. On the other hand, shrouding compared with the standard HVOF torch decreased particle speeds, and as a result coating porosity was higher. Based on the previous experiences and analyses, a new nozzle attachment was numerically modeled, designed, and used to produce various thermal spray coatings. This article presents a combined numerical and experimental investigation of the process. In-flight particle con-

The original version of this article was published as part of the ASM Proceedings, *Thermal Spray 2003: Advancing the Science and Applying the Technology*, International Thermal Spray Conference (Orlando, FL), 5-8 May, 2003, Basil R. Marple and Christian Moreau, Ed., ASM International, 2003.

A. Dolatabadi, Mechanical and Industrial Engineering Department, Concordia University, Montreal, Quebec, Canada, **V. Pershin** and **J. Mostaghimi,** University of Toronto, Toronto, Canada. Contact e-mail: pershin@mie.utoronto.ca.

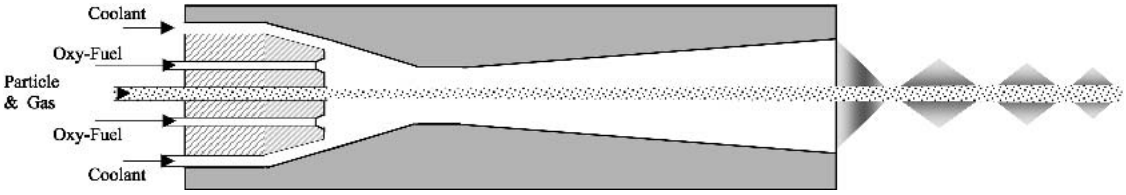

Fig. 1 Schematic diagram of a typical HVOF nozzle

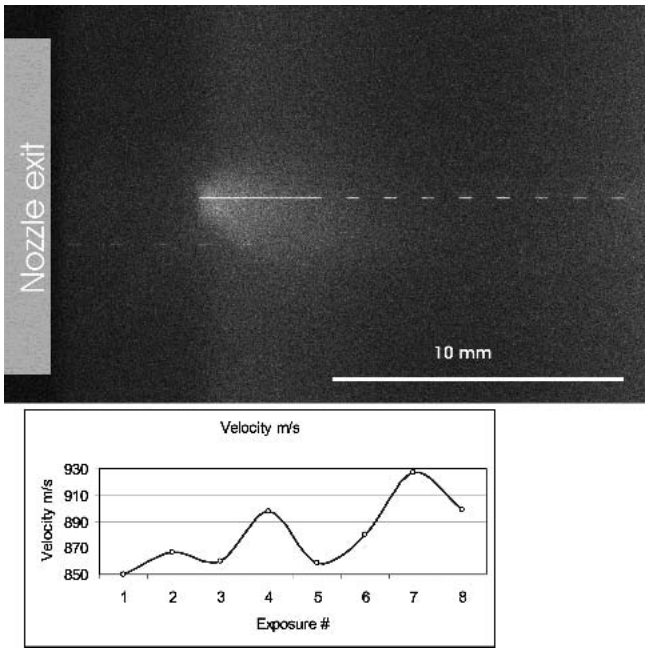

Fig. 2 ZrO_2 particle trajectory and its velocity fluctuation in the vicinity of the first shock; exposure 500 μs, delay 1000 μs

ditions for the cases with and without the shroud are compared, and samples of coatings using the new nozzle are presented.

2. Shock Waves in HVOF Spraying

The motivation for designing the new nozzle was based on the gas dynamic that governs the supersonic flow generated in the HVOF process. As explained previously, the HVOF gun is basically a converging-diverging nozzle to accelerate the gas flow to supersonic speeds at the gun exit. At the end of the gun, the flow is overexpanded; that is, the Mach number is greater than one and gas pressure is lower than that of the ambient atmosphere. Because the flow is supersonic, the adjustment to the atmospheric pressure is through a series of oblique shocks and expansion waves, called shock diamonds (Fig. 3). This pattern will be repeated until the gas pressure reaches ambient pressure. In an HVOF process, up to nine shock diamonds may form in the ambient air.

The main advantage of the HVOF process is to generate supersonic flows by which particles can reach high velocities. The reason is that for highly compressible flows the relative velocity between gas and particle can be greater than the local sound

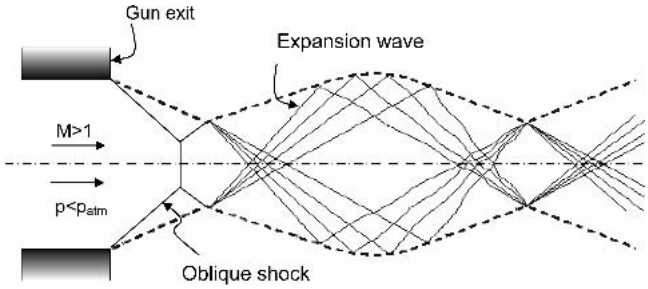

Fig. 3 Formation of the first shock

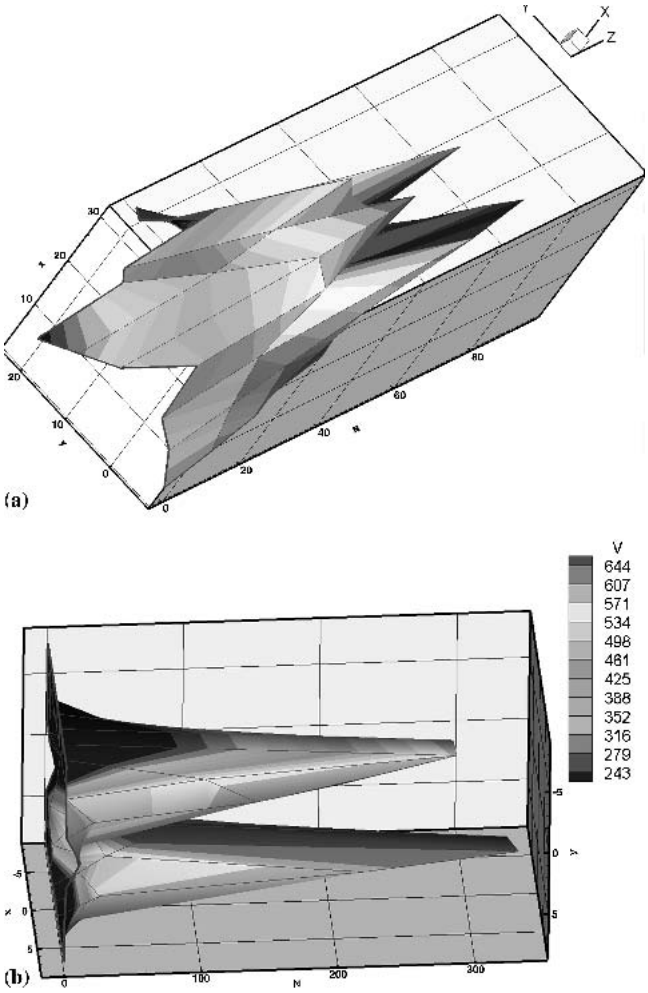

Fig. 4 Velocity and particle No. distribution of (a) spherical Diamalloy 1003 and (b) nonspherical Metco 45VF-NC powders at spraying distance of 100 mm using DJ gun

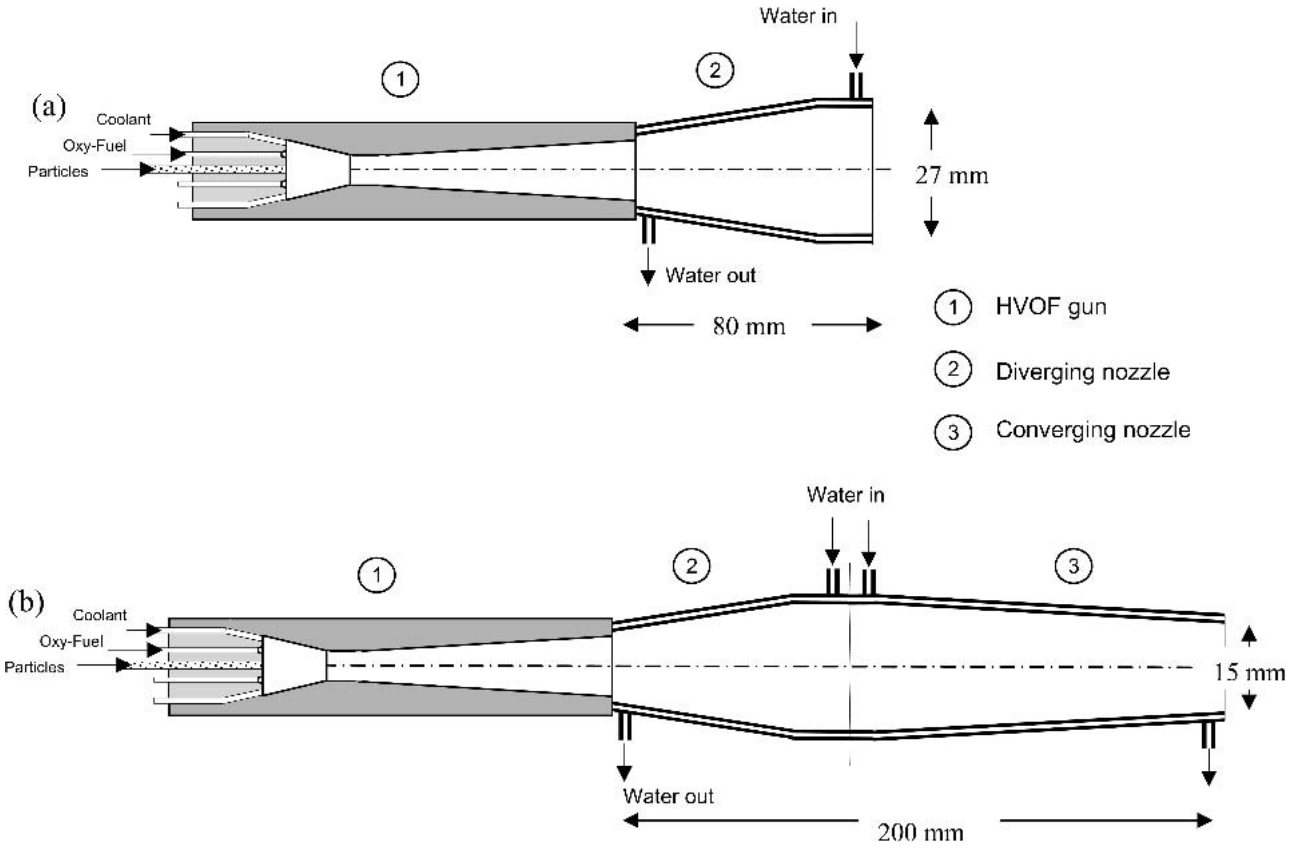

Fig. 5 Attachment configurations. (a) Diverging. (b) Diverging-converging

speed. In this case, the compression shocks forming in front of a particle can accelerate it to higher velocities; this is known as a wave drag effect (Ref 11). For the internal flow (i.e., inside the gun), almost a uniform flow exists at each cross-sectional area of the gun. Outside the gun, the external flow becomes totally different due to formation of a series of shocks and expansion waves. The interaction of an oblique shock and expansion wave with a passing particle, presented in Fig. 2, clearly shows a large fluctuation of the ZrO_2 particle velocity on travel distance of less than 10 mm. Essentially, particles gain kinetic and thermal energy from the gas flow; as a result, particle conditions such as velocity, temperature, and trajectory are strongly dependent on the flow behavior. In the free jet flow, particles repeatedly are accelerated and decelerated while passing through the shock diamonds formed outside the nozzle (Ref 12). Moreover, analysis of the images of moving particles through the first shock shows that the particles also deviate from their trajectories (which are ideally parallel to the nozzle centerline) due to gas flow fluctuations.

In experimental measurements of particles conditions using a DPV-2000 system (Tecnar Ltee, St-Bruno, Canada) (Ref 13); instead of focusing only on the centerline, the sensor scanned the whole cross-sectional area with 2 mm steps. The results of scanning a particle flow formed by the standard DJ HVOF gun at a stand-off distance of 100 mm is shown in Fig. 4. A bimodal spatial distribution of spherical particles (Diamalloy 1003, Sulzer-Metco Inc., Westbury, NY) can be observed in Fig. 4(a). It clearly shows that there is a smaller number of particles near the centerline where the maximum particle velocity zone exists. Most of the particles deviate due to passing through a series of oblique shock and expansion waves. Combination of the particle deceleration and the effect on its trajectory deviation prevents it from reaching velocities required for adhering to the substrate, and quality can be negatively affected. An unusual and more unfavorable particle distribution (Fig. 4b) was observed for the powder with nonspherical particles (Metco 45VF-NC, Sulzer-Metco Inc.). Nozzle rotation of the gun on 90° did not change such asymmetric distribution of the particles. This could be a result of the number of combined aspects, namely shock influence, wear of a powder injector, or misalignment internal parts of the gun. Shop users without a particle monitoring system should be aware of the existence of such a scenario as a factor affecting inconsistent quality of coatings from run to run.

3. Nozzle Design and Modeling

The basic concept behind the design of the new nozzle attachment was to eliminate the shock diamonds and let the gas flow have a smooth transition from supersonic to subsonic flow. The schematic illustration of the attachment (Ref 14) to the HVOF gun is shown in Fig. 5. It can be used in two modes depending on the applications: diverging (D) or diverging-converging (D-C); each section is water-cooled (Fig. 5). Water flow rate through the attachment was 21 L/min.

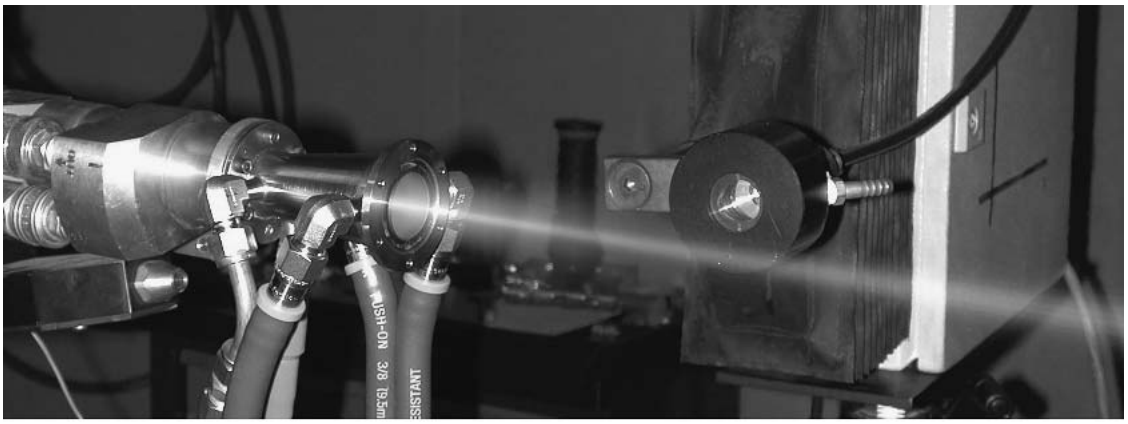

(a)

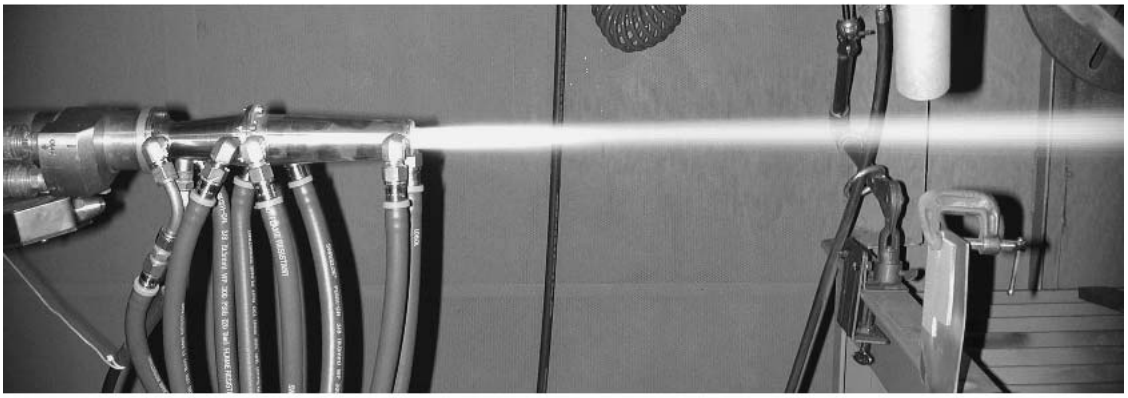

(b)

Fig. 6 (a) Diverging and (b) diverging-converging attachments in operation

To evaluate the effect of the attachment, prior to the experiments, a numerical analysis was performed for the flow conditions with and without the attachment using numerical methodology presented in Ref 10. The Eulerian formulation for the gas and Lagrangian approach for particle tracking was used. Combustion was modeled by a multireaction eddy dissipation model (EDM) that included the dissociation of the combustion products.

4. Experimental Conditions

To study the performance of the new nozzle, experiments were carried out using DJ-2700 HVOF torch (Sulzer-Metco Inc.) with propylene as fuel. Only the D-C or D part of the attachment were fastened to the gun (Fig. 6) and tested. The experiments with the free jet and the attachment were performed under the same operating conditions. The standoff distance for all cases was measured from the standard HVOF nozzle exit. In-flight particle conditions such as velocity, temperature, and size were measured with a DPV-2000 monitoring system. A high-speed charge coupled device (CCD) camera (SensiCam, Opticon Corp., Kitchener, ON, Canada) was used to capture images for evaluation of the effect of shock diamonds on deceleration and deviation of individual particles.

Table 1 Particle velocity and temperature comparison for free jet and D-C attachment

45VF-NS powder ($Co_{25}Cr_{10.5}Ni_{7.5}W$ particle size −45 +5 μm)	Free jet (standoff distance), mm		D-C attachment (standoff distance), mm	
	200	300	200	300
Velocity, m/s	576 ± 106	470 ± 72	736 ± 98	609 ± 76
Temperature, °C	2029 ± 159	2064 ± 143	1896 ± 149	2034 ± 125

The jet gas composition was measured using a mass-spectrometer (Microvision Plus, MKS Instrument, Crewe, UK). The spectrometer inlet capillary was equipped with a ceramic tip and was placed along the torch centerline.

5. Results and Discussion

5.1 Metallic Coatings

The numerical results are presented in Fig. 7 and 8. They provide comparison of the main flow features calculated for configurations with and without the attachment. The rapid release of energy near the oxyfuel inlet causes increase in temperature, resulting in a considerable decrease in density and an increase in

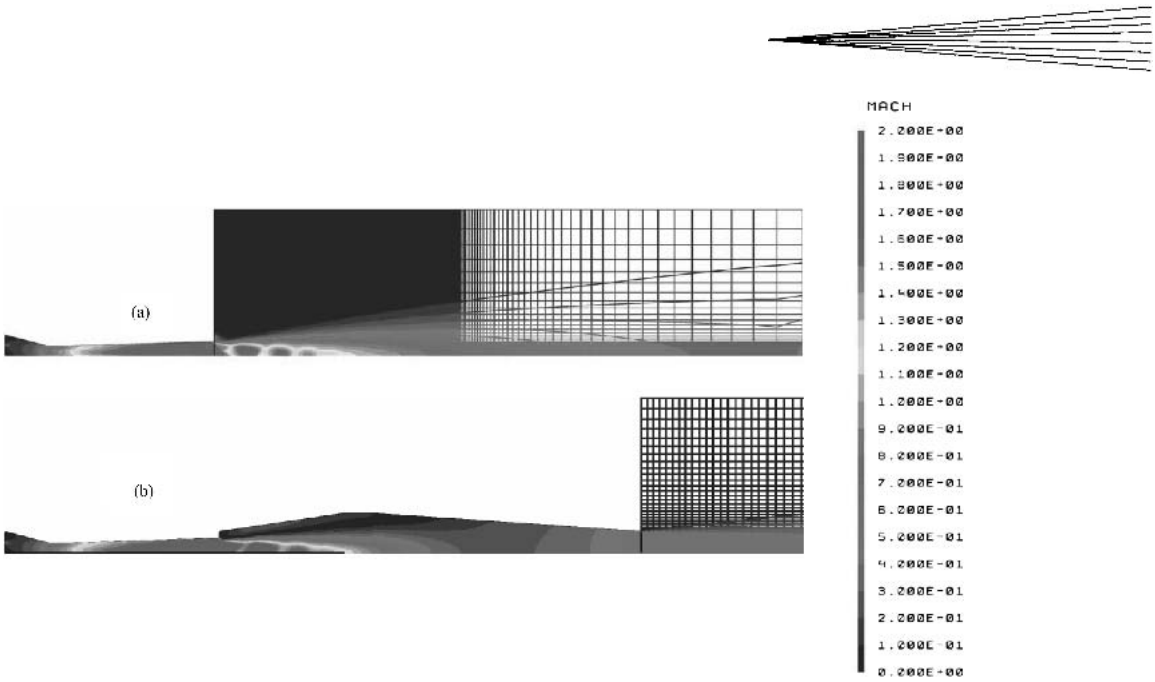

Fig. 7 Mach number contours. (a) Free jet. (b) D-C attachment

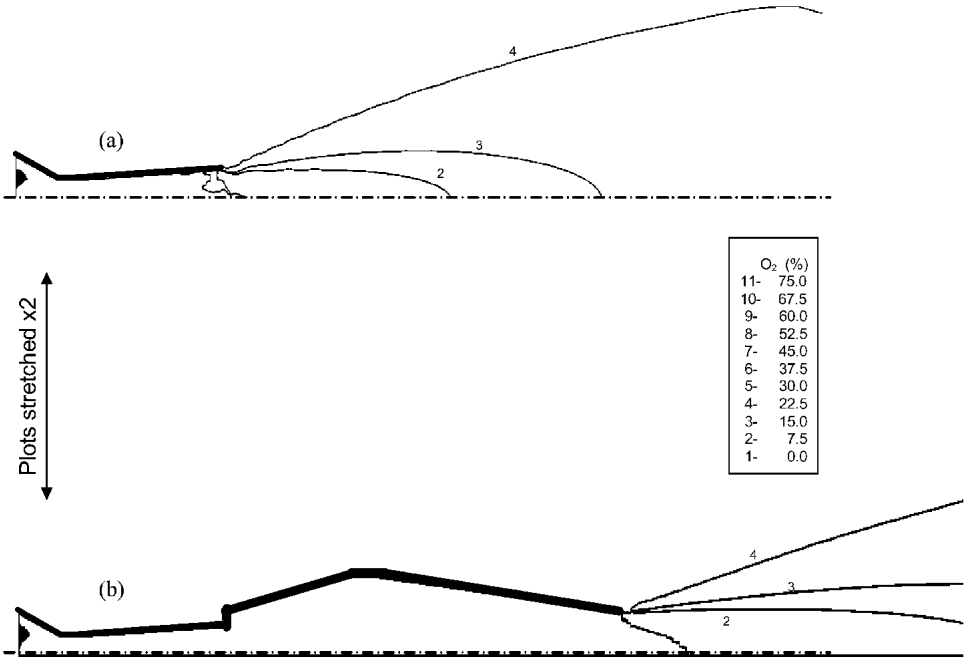

Fig. 8 Oxygen concentration. (a) Free jet. (b) D-C attachment

pressure. This generates high velocities near the inlet and the supersonic flow develops inside of the gun. Since the flow is supersonic at the gun exit, the characteristics of the flow inside the gun are nearly the same for both cases, with and without the attachment. The overexpanded flow produces shock diamonds outside the gun for the free jet case. With the D-C attachment to the gun, the region with supersonic flow is extended further outside the nozzle, and transition from supersonic to subsonic flow is no longer through shock diamonds (Fig. 7).

The D-C attachment provides a transition from supersonic to subsonic flow much smoother than that of the free jet case. Two effects, diminishing the shock diamonds and extending the supersonic flow, associated with the flow in the new configuration, result in less particle deviation and more efficient particle acceleration than those of the free jet. In addition, the attachment reduces the entrainment of ambient air into the main stream. This effect is evident when Fig. 8(a) and (b) are compared. Oxygen concentration at the spraying position reduces from about 20% for the case of free jet, to less than 3% for the case with the D-C attachment. Therefore, protecting the main stream from entrain-

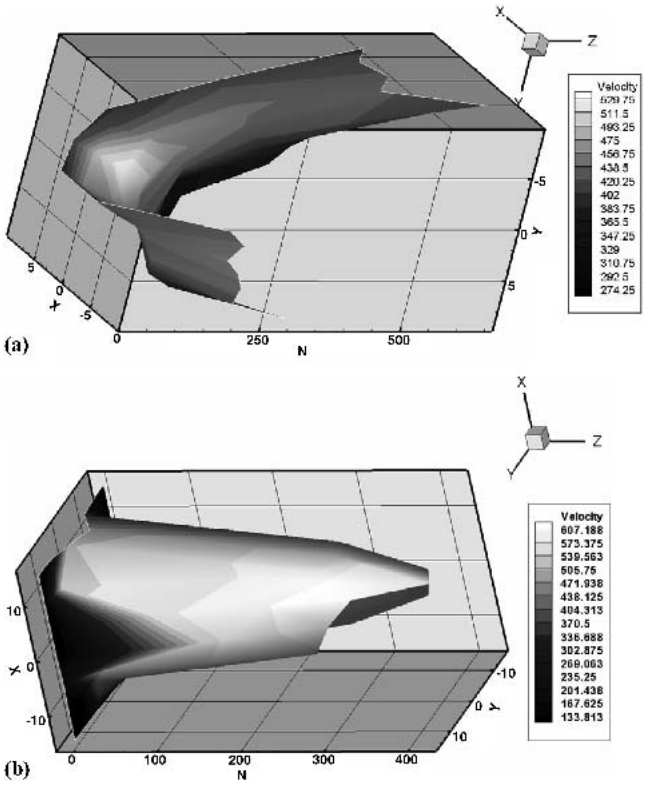

Fig. 9 Particle number (*Z*-axis) and velocity distribution of Mecto 45VF-NC powder at spray distance 300 mm. (a) Free jet. (b) D-C attachment

ment of the ambient air may significantly reduce the oxide formation in the coating.

The results of measurements at standoff distances of 200 and 300 mm for cobalt (Co) alloy powder (45VF-NS) are presented in Table 1.

Particle velocity, which is a key parameter in producing high-density coating, increases up to 30% with the D-C attachment. Although the new nozzle provides a higher gas temperature field, particle temperature is lower relative to the free jet, which can be correlated to in-flight particle oxidation. The D-C attachment delays air entrainment into the jet, which reflects in reduced particle oxidation. Measured oxygen content for this powder shows that in a coating deposited with standard gun, average level is 2.15 wt.%, whereas for that deposited with the D-C attachment, it is 1.59 wt.% . The shrouding effect diminishes as the standoff distance increases, and at a standoff distance of 300 mm particle temperature rises with no heat sources other than the oxidation.

The effect of the D-C attachment could be seen in results of simultaneous analysis of the particle spatial distribution and condition; the number of scans of the free jet and gun with the attachment were carried out using the DPV system at various spray distances. In particular, measurements of particle conditions in a plane perpendicular to the jet direction were carried out at 81 points with steps of 2 mm. Figure 9 shows the results of such measurement of the Metco 45VF-NC powder velocities versus the number of the particles during spraying with and without the D-C attachment at a standoff distance of 300 mm. The flow produced by the new nozzle provides a favorable particle distribution and results in higher particle average velocities across the jet compared with those of the free jet. Moreover, only a few particles reached maximum velocity in the free jet case, whereas with the jet emerging from the D-C attachment, the majority of the particles reached maximum velocity.

The measurements also revealed that using only the diverging attachment in comparison with the free-jet causes reduction in oxygen and increase of hydrogen concentration of the jet (Table 2).

Figure 10 shows the microstructure of a Co-based coating produced with the D-C and D attachments and the standard gun at 300 mm standoff distance. Dense concentration of particles in the central zone of the jet generated by the gun with an attachment and their higher velocities are beneficial for the coatings quality as well as the coating/substrate interface. The same result was achieved for WC-17Co (Diamalloy 2005, Sulzer-Metco Inc.) coatings where the D attachment provided a uniform low-porosity coating.

5.2 Ceramic Coatings

Finally, using the attachment enabled the authors to apply low-porosity alumina coatings with a deposition rate appropriate for industrial applications. As mentioned earlier, the particle trajectories are better controlled with the attachment resulting in higher particle velocities and more uniform temperatures. Such combination of parameters is one of the major factors that allow deposition of materials with high melting points, such as alumina.

The Al_2O_3 particle discharging through the D attachment showed that the average particle temperature was almost unaffected by increasing the powder loading from 10 to 30 g/min; only the average velocity decreased from 690 to 630 m/s. Although the average particle temperature is still below the melting point, specification of gas and particle flow in the attachment provides heating up to the maximum available temperatures for large amounts of particles. As a result, this increases deposition efficiency of the alumina powder and makes HVOF process feasible for coating deposition. Microstructure observation (Fig. 11) also revealed that alumina coating has two distinct phases, unmelted or semimolten particles surrounded by a glasslike, dense matrix of fully molten phase. The two-phase structure was also confirmed by x-ray diffraction analysis (Fig. 12). It consists of predominantly αAl_2O_3 phase, which may be correlated to unmelted particles, since the initial powder had α-phase only. The second phase was γAl_2O_3, which is usually formed from molten Al_2O_3 during rapid solidification. This differs from plasma spraying of alumina, where coatings are generally formed by completely molten particles producing a structure composed mostly of γAl_2O_3 with poorer service performance. Due to high impact velocity, the alumina coating porosity was less than 2%. From this perspective, use of the attachment will be specifically beneficial for deposition of nanostructured ceramic powders when preservation of the initial structure of the powders is essential.

6. Summary and Conclusions

The results and findings from the numerical analysis were used to design a new attachment for the HVOF torch. The ob-

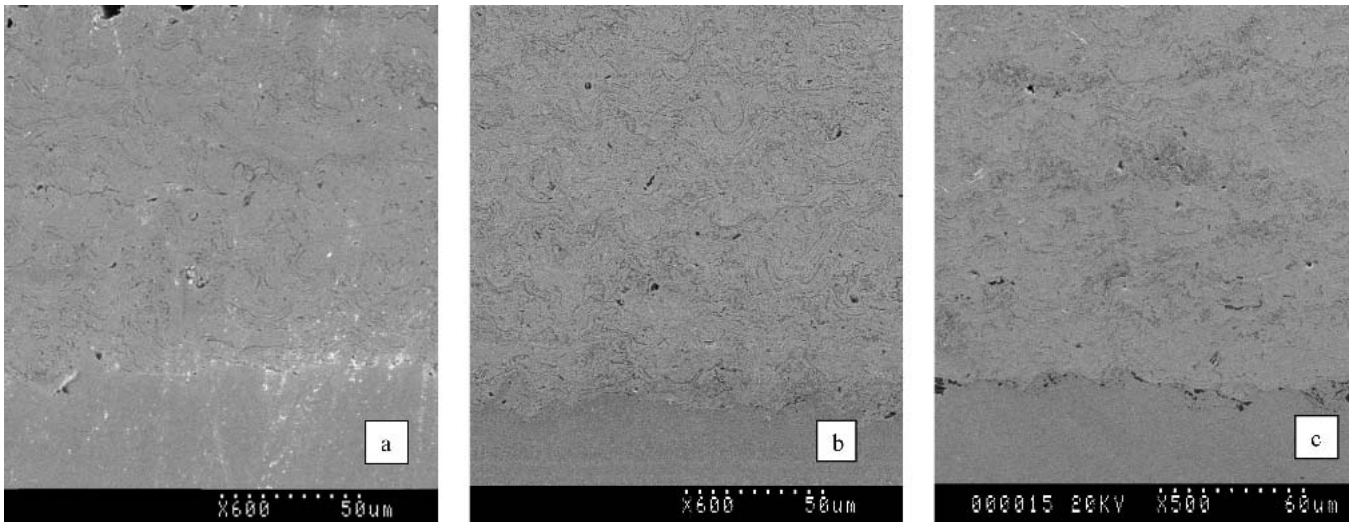

Fig. 10 Co-based coating microstructure with (a) D-C and (b) D attachments and (c) standard torch

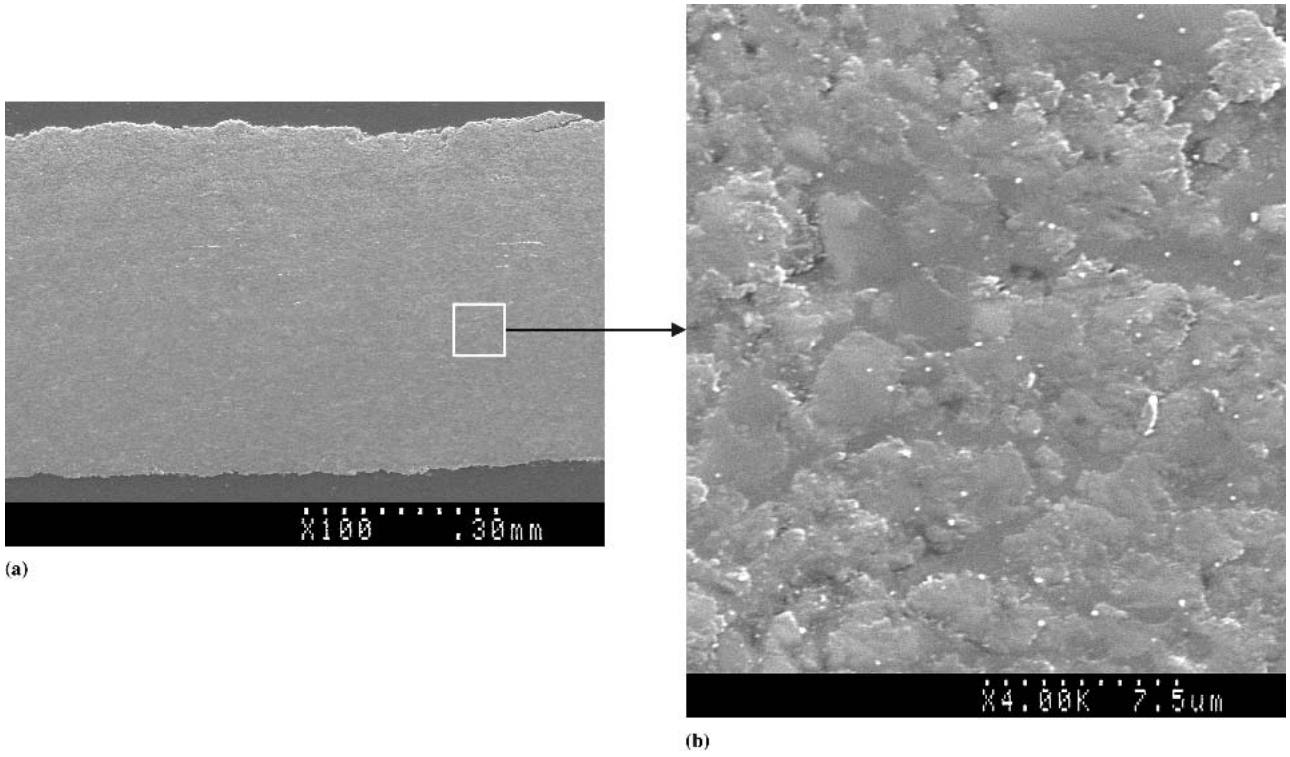

Fig. 11 Microstructure of Al_2O_3 coating deposited by D-C attachment. (a) 100×. (b) 4000×

jective was to improve the performance of the coating process according to the needs of industry, such as increased deposition efficiency, minimized in-flight oxidation, and flexibility to allow coating of ceramic powders. Conclusions from the numerical and experimental evaluations are summarized as follows:

Formation of several shocks and expansion waves outside of the HVOF gun results in particles deceleration and deviation of their trajectory. The basic concept behind the new attachment was to substantially reduce or eliminate the shock diamonds associated with the standard HVOF nozzles so that the gas flow has a smoother transition from supersonic to subsonic flow.

Similar to the cylindrical shroud, the new attachment is able to prevent the penetration of the ambient air into the main spray flow and reduce in-flight oxidation of particles. The experimental measurements of gas composition, in agreement with numerical simulations, showed favorable changes

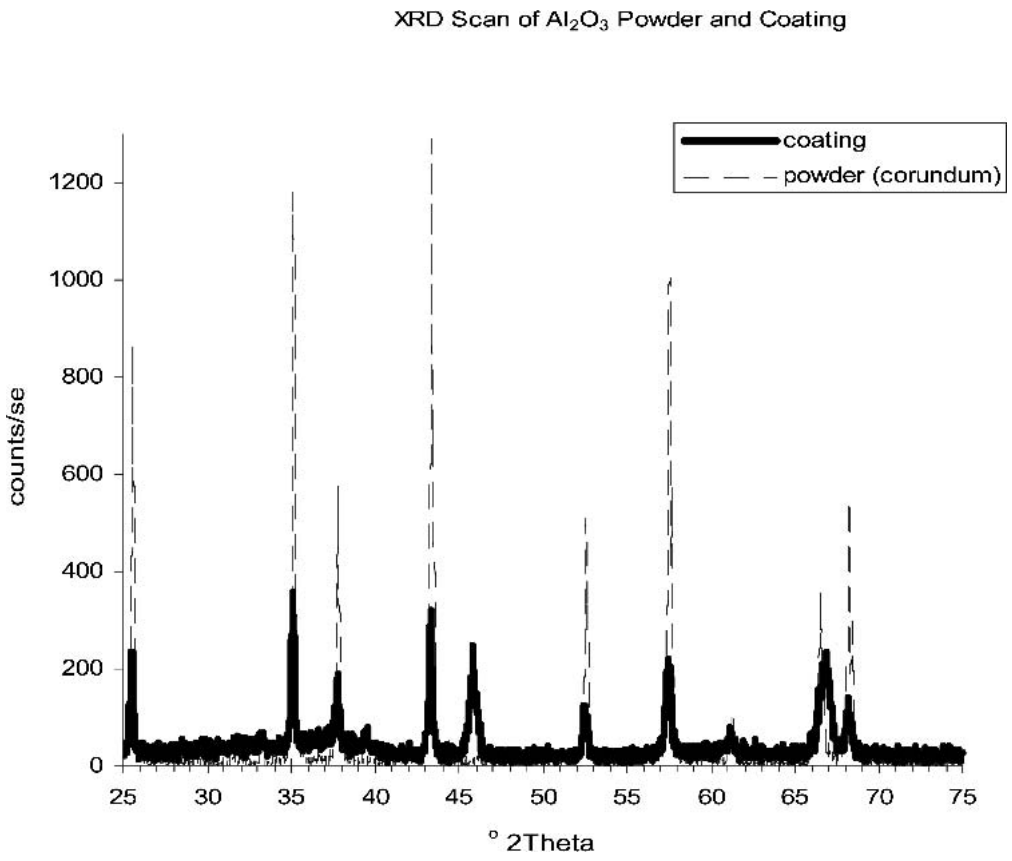

Fig. 12 XRD analysis of initial Al_2O_3 powder and coating applied by D-C attachment

Table 2 Gas composition for the cases with and without the attachment

	Free jet (% of total pressure)		Diverging attachment (% of total pressure)	
	230 mm	**230 mm**	**250 mm**	**300 mm**
Water	60.05	50.31	53.99	56.11
Nitrogen	25.03	23.30	24.42	26.79
Oxygen	6.06	2.94	4.43	5.47
Hydrogen	0.33	2.26	0.59	0.30
Others (CO_2,NO, etc.)	8.53	21.19	16.57	11.33

in reduction-oxidation potential of the jet protected by the attachment.

Performance of the new attachment in two configurations was investigated by spraying various coating materials including metallic, carbide, and oxide powders. Particle spatial distribution, velocity, and temperature for the torch with and without the attachment were compared. The attachment provides a favorable particle spatial distribution, as well as higher and more uniform particle velocity and temperature. These improvements enable spraying of dense Al_2O_3 coating with porosity less than 2%.

Experiments also revealed that a pointwise measurement at each standoff distance cannot provide complete information on particle conditions. However, by mapping the cross section of the entire jet, the spatial distribution, along with particle velocity and temperature can be examined. In particular, the bimodal spatial distribution of the particles for the standard HVOF torch was observed by this method.

Acknowledgment

This work was supported by the Natural Sciences and Engineering Research Council of Canada (NSERC), Materials and Manufacturing Ontario (MMO), and the member companies of the Thermal Spray Consortium at the University of Toronto.

References

1. W. Brandl, D. Toma, J. Kruger, H.J. Grabke, and G. Matthaus, The Oxidation Behaviour of HVOF Thermal-Sprayed MCrAlY Coatings, *J. Surf. Coat. Technol.,* Vol 94-95, 1997, p 21-26
2. E. Lugscheider, C. Herbst, and L. Zhao, Parameter Studies on High-Velocity Oxy-Fuel Spraying of MCrAlY Coatings, *J. Surf. Coat. Technol.,* Vol 108-109, 1998, p 16-23
3. G. Irons and V. Zanchuk, Comparison of MCrAlY Coatings Sprayed by HVOF and Low Pressure Processes, *Thermal Spray Coatings: Research, Design and Applications,* C.C Berndt and T.F. Bernecki, Ed., ASM International, 1993, p 191-197
4. D. Toma, W. Brandl, and U. Koster, Studies on the Transient Stage of Oxidation of VPS and HVOF Sprayed MCrAlY Coatings, *J. Surf. Coat. Technol.,* Vol 120-121, 1999, p 8-15
5. L. Russo and M. Dorfman, High Temperature Oxidation of MCrAlY Coatings Produced by HVOF, *Thermal Spray Science and Technology,* C.C. Berndt, Ed., ASM International, 1995, p 1179-1184

6. L.N. Moskowitz, Application of HVOF Thermal Spraying to Solve Corrosion Problems in the Petroleum Industry, *Thermal Spray: International Advances in Coatings Technology,* C.C. Berndt, Ed., ASM International, 1992, p 611-618
7. C.M. Hackett and G.S. Settles, Research on HVOF Gas Shrouding for Coating Oxidation Control, *Thermal Spray Sci. Technol.,* C.C. Berndt and S. Sampath, Ed., ASM International, 1995, p 21-29
8. L. Moskowitz and D.J. Lindley, U.S. Patent No. 5, 019, 426
9. V. Pershin, J. Mostaghimi, S. Chandra, and T. Coyle, A Gas Shroud Nozzle for HVOF Spray Deposition, *Thermal Spray: Meeting the Challenges of the 21st Century,* C. Coddet, Ed., ASM International, 1998, p 1305-1308
10. A. Dolatabadi, J. Mostaghimi, and V. Pershin, Effect of a Cylindrical Shroud on Particle Conditions in High Velocity Oxy-Fuel (HVOF) Spray Process, *Sci. Technol. Adv. Mater.,* Vol 3, 2002, p 245-255
11. M.J. Walsh, Drag Coefficient Equation for Small Particles in High Speed Flows, *AIAA J.,* Vol 13 (No. 11), 1975, p 1526-1528
12. A. Dolatabadi, V. Pershin, and J. Mostaghimi, Effect of Flow Regime on Particle Velocity in the High Velocity Oxy-Fuel (HVOF) Process, *Tagungsband Conference Proceedings,* E. Lugscheider, Ed., DVS, Germany, 2002, p 918-925
13. C. Moreau, P. Gougeon, M. Lamontagne, V. Lacasse, G. Vaudreuil, and P. Cielo, On-line Control of the Plasma Spraying Process by Monitoring the Temperature, Velocity and Trajectory of In-flight Particles, *Thermal Spray Industrial Applications,* C. Berndt and S. Sampath, Ed., ASM International, 1994, p 431-437
14. A. Dolatabadi, J. Mostaghimi, and V. Pershin, High Efficiency Nozzle for Thermal Spray of High Quality, Low Oxide Content Coatings, US Patent US-2003-0178511-A1, filed March 2002